ChemComm

Accepted Manuscript

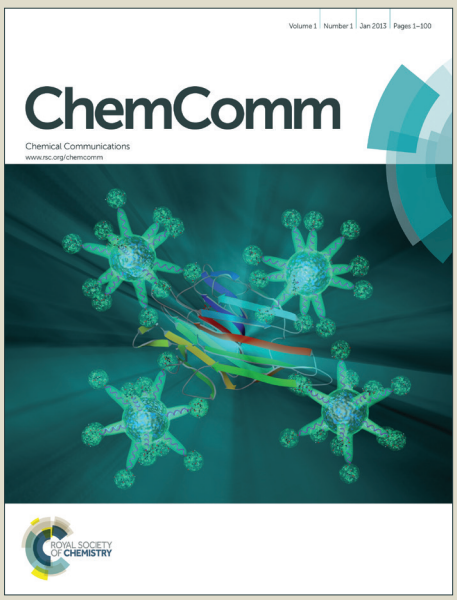

ROYAL SOCIETY OF CHEMISTRY

www.rsc.org/chemcomm

Journal Name

RSCPublishing

COMMUNICATION

Live imaging of cellular dynamics using a multi-imaging vector in single cells†

Cite this: DOI: 10.1039/x0xx00000x

Kyoungsook Park,‡ [a] Jinyoung Jeong‡[a,b] and Bong Hyun Chung*[a,b]

Received 00th January 2012,
Accepted 00th January 2012

DOI: 10.1039/x0xx00000x

www.rsc.org/

Real-time monitoring of cellular dynamics in living organisms is highly challenging. We developed a multi-imaging vector based on 2A peptides. Live imaging of subcellular compartments can be performed following the transfection of cells with another vector, the multi-labeling vector, which contains localization signals and various fluorescent protein variants.

Visualizing the complexity and dynamics of cellular events in living cells is important for understanding biological processes, such as normal physiology and disease progression. Multi-gene expression systems, which simultaneously generate more than two target proteins, offer a powerful tool for cellular imaging. For example, internal ribosomal entry site (IRES) vectors have been widely used to express two individual proteins in mammalian cells.[1] Recently, a Gal4-dependent multicistronic expression system based on triple and quadruple Medusa vectors has been developed to monitor subcellular dynamics in developing zebrafish.[2] However, these approaches have drawbacks, including low efficiency, disproportionate protein expression, and the requirement of a secondary vector as an initiator.[3]

Here, we report a multi-imaging vector for real-time monitoring of cellular dynamics using the 2A peptide system, allowing the expression of multiple proteins within a single open reading frame (ORF) via a self-cleaving event. 2A peptides consist of 18-22 amino acid long peptide, including short consensus sequences (Asp-Val/Ile-Glu-X-Asn-Pro-Gly-Pro); this sequence is cleaved between the Gly and Pro residues by a ribosomal skip mechanism.[4] These peptides are used to generate multiple proteins from single transcripts by several RNA viruses, such as foot-and mouth disease virus (FMDV), equine rhinitis A virus (ERAV), the insect Thosea asigna virus (TaV), and the porcine teschovirus-1 (PTV-1).[4,5] In the ribosomal skip mechanism, proteins become separated when a normal peptide bond fails to form during translation at the cleavage point, without affecting the translation of following proteins. Although the 2A peptide system is widely used to express multicistronic products in developmental biology during the generation of transgenic animal models.[6-8] this system has rarely been used as a cellular imaging tool. Therefore, we developed a multi-imaging technique based on the 2A peptide system to monitor cellular dynamics in a live cell. First, we designed and constructed a multi-imaging vector that included commonly used restriction enzyme sites and three distinct 2A peptides (named F2A from FMDV, T2A from TaV, and E2A from ERAV) to simultaneously express four proteins (Scheme. 1a). This combination of restriction enzyme sites and 2A peptides was synthesized, and the original multiple cloning site of the pcDNA4/HisMax. A backbone vector was then replaced with this construct to generate a multi-imaging vector (Scheme. 1b). While attempting to image a live cell at the subcellular level, we designed a multi-labeling vector based on the multi-imaging vector (Fig. 1a). The multi-labeling vector consists of four distinct fluorescent protein variants, including enhanced cyan fluorescent protein (ECFP), enhanced green fluorescent protein (EGFP), Discosoma red fluorescent protein2 (DsRed2), and infrared fluorescent protein670 (iRFP670).[9] These fluorescent proteins were selectively chosen to avoid overlapping excitation/emission spectra for distinct subcellular imaging (Table S1, ESI†).

[a] *BioNano Health Guard Research Center, Korea Research Institute of Bioscience and Biotechnology (KRIBB)*

[b] *Nanobiotechnology Major, School of Engineering, University of Science and Technology (UST) , 125 Gwahangno, Yuseong, Daejeon 305-806, Republic of Korea.*
E-mail: chungbh@kribb.re.kr; Fax: +82-42-879-8594; Tel: +82-42-860-4442

† Electronic Supplementary Information (ESI) available: Experimental details and supplementary data. See DOI: 10.1039/c000000x/

‡ These authors contributed equally to this work.

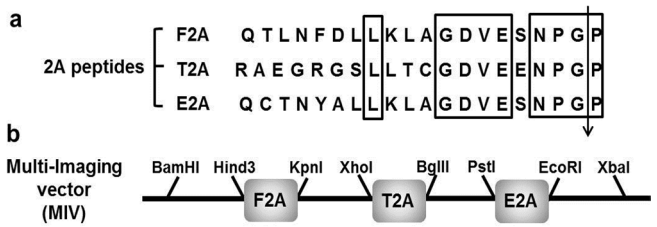

Scheme 1 Construction of the multi-imaging vector and subcellular imaging using the multi-labeling vector. (a) Amino acid sequence of the 2A peptides F2A, T2A, and E2A. The cleavage site is indicated by an arrow, and conserved sequences are surrounded by boxes. (b) Design of multi-imaging vector constructs.

To target specific organelles, the fluorescent proteins were fused to well-known localization signals. We fused a mitochondrial targeting sequence derived from subunit VIII of human cytochrome C oxidase[10] to the N-terminus of DsRed2 (termed Mito-DsRed2) (Fig. S1, ESI†) and an endosomal targeting protein from human RhoB GTPase[11,12] to the N-terminus of EGFP (termed EGFP-Endo) (Fig. S2, ESI†). We also attached three copies of the nuclear localization signal (NLS) from simian virus 40 large T-antigen[13] to the C-terminus of ECFP (termed ECFP-NLS) and attached the membrane localization sequence of neuromodulin[14] to the N-terminus of iRFP670 (termed Memb-iRFP670).

To validate the expression of each of these subcellular localized fluorescent proteins, we transfected the multi-labeling vector into HeLa cells. After transfection, confocal images showed the multi-expression of the fluorescent proteins in their respective targeting compartments in a single cell (Fig. 1b). These images revealed that each fluorescent signal was consistently localized (Fig. 1c; DsRed2 in mitochondria, EGFP in endosomes, ECFP in the nucleus, and iRFP670 in the membrane). The localization was confirmed by immunofluorescence using early endosomal marker (EEA1) for fo-staining of EGFP-Endo as an example (Fig. S4, ESI†). Interestingly, it appeared that the C-terminal addition of the 2A fragment did not affect the subcellular localization of the fluorescent proteins, indicating the possibility of simultaneously expressing multiple cellular-labeled fluorescent proteins in a single cell.

Subsequently, we explored using the multi-imaging vector to track target proteins during biological processes. We generated a multi-monitoring system to monitor the redistribution of apoptosis-inducing factor (AIF) and Bcl-2 associated X protein (Bax) during programmed cell death (PCD) in a single cell. Upon the induction of apoptosis, the mitochondrial intermembrane flavoprotein AIF is translocated from the mitochondria to the nucleus to participate in large-scale DNA fragmentation and chromatin condensation as a proapoptotic factor in a caspase-independent pathway.[15,16] AIF is known to be a key player in cell death mechanisms under various pathological conditions, including ischemic injury, cancers, and neurodegenerative disorders. More recently, Bax-mediated mitochondrial release of AIF has been shown to be a critical step in PCD. Bax promotes apoptosis by antagonizing the Bcl-2 protein. The redistribution of Bax from the cytosol into the mitochondria has been found to be important for the ability of Bax to promote cell death during apoptosis.[17] According to recent reports, activated Bax

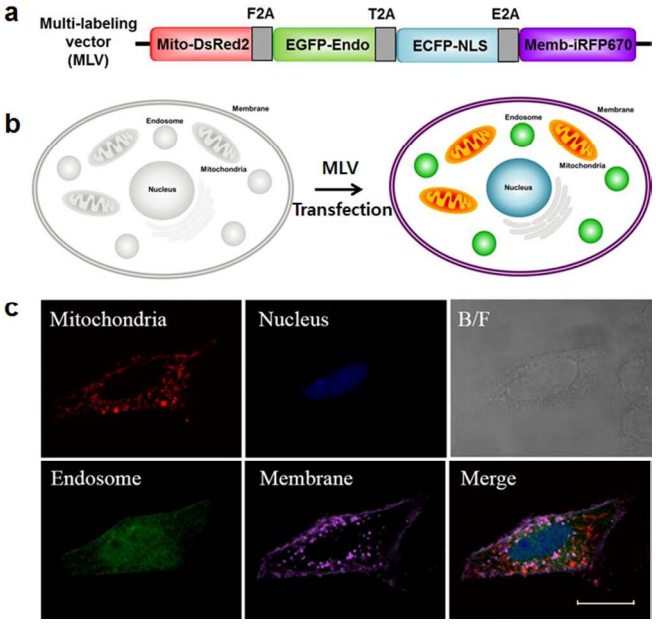

Fig. 1 (a) Schematic representation of the multi-labeling vector for subcellular imaging, which is based on the multi-imaging vector. A multi-labeling vector containing subcellular labels for mitochondria (Mito-DsRed2, red), endosome (EGFP-Endo, green), nucleus (ECFP-NLS, blue), and membrane (Memb-iRFP670, purple). (b) Illustration of a cell transfected with the multi-labeling vector. (c) Fluorescent images of HeLa cells expressing a multi-labeling vector. DsRed2 labeled the mitochondria in red; EGFP labeled the endosome in green; ECFP labeled the nucleus in blue; and iRFP670 labeled the membrane in purple. Scale bar = 20 μm.

induces outer mitochondrial membrane permeabilization and allows AIF to be released into the cytosol.[18,19]

Although efforts have been made to discover the mechanism of AIF and the relationship between AIF and Bax in PCD, the mitochondrial permeabilization event still remains unclear, especially during caspase-independent PCD. To elucidate the mechanisms underlying mitochondrial permeabilization, general protocols, such as differential cell-permeabilization, submitochondrial fractionation, and immunostaining, have been developed.[20,21] However, the development of a real-time monitoring approach is necessary to monitor cellular dynamics. Therefore, we designed a multi-monitoring vector to detect the AIF-Bax redistribution. As described in Fig. 2a, we fused EGFP to the C-terminus of AIF (termed AIF-EGFP) and iRFP670 to the C-terminus of Bax (termed Bax-iRFP670). EGFP-Endo and Memb-iRFP670 in the multi-labeling vector were then replaced with AIF-EGFP and Bax-iRFP670, respectively.

Monitoring of the AIF-Bax redistribution was performed using HeLa cells, which underwent staurosporine (STS)-induced apoptosis after transfection with a multi-monitoring vector. STS, an alkaloid from a Streptomyces species, is known to be a strong apoptosis inducer in several cell types, including HeLa cells. After transfection, cells were exposed to 5 μM STS for 5 hrs and then observed under confocal microscopy to monitor the fluorescent signals. Fig. 2b shows the time-dependent fluorescence signals from HeLa cells bearing the multi-monitoring vector. There was no indication of AIF

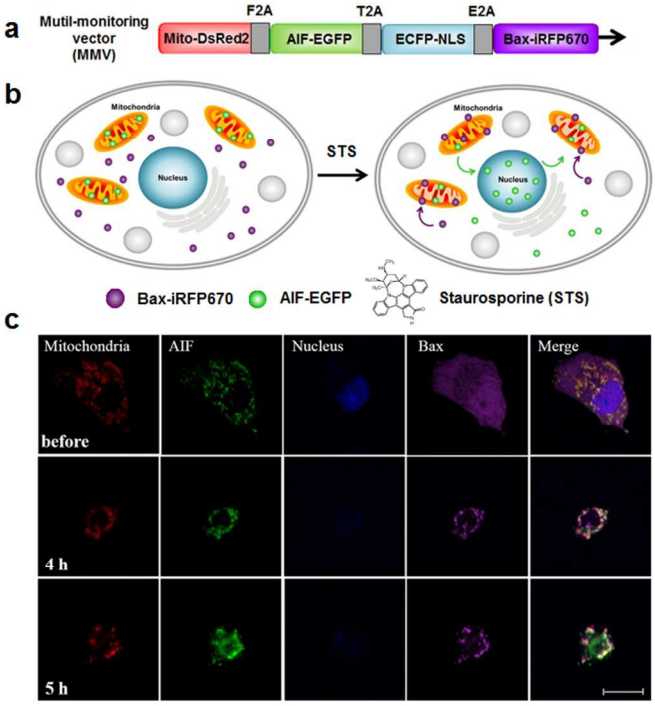

Fig. 2 Multi-monitoring system for examining AIF-Bax redistribution during apoptosis. (a) Design of the multi-monitoring vector for the detection of apoptotic protein trafficking. (b) Illustration of the redistribution of AIF and Bax following the induction of apoptosis by STS treatment. (c) Fluorescent images of target protein translocation in HeLa cells transfected with the multi-monitoring vector. After transfection, HeLa cells were treated with 5 μM STS for 5 hrs. Bax was labeled with iRFP670 in purple, and AIF was labeled with EGFP in green. DsRed2 labels the mitochondria in red, and ECFP labels the nucleus in blue. Scale bar = 20 μm.

or Bax translocation in cells until 3 hrs after STS treatment. The purple fluorescence of Bax-iRFP670 was detectable in the mitochondria but not in the cytosol 4 hrs after STS exposure.

The green fluorescence of AIF-EGFP was observed in both the cytosol and nucleus 5 hrs after STS treatment. In cells that were not treated with STS, AIF and Bax were localized to the mitochondria and cytosol, respectively. Upon the induction of apoptosis by STS, Bax was found in the mitochondria, whereas a large portion of AIF was translocated into the nucleus (Fig. 2c). Similar results were obtained with another anticancer drug (0.5 mM etoposide) after cells were exposed for 6 hrs (Fig. S5, ESI†), indicating that this system is able to monitor the cellular dynamics of protein translocation induced by an apoptotic stimulus. Moreover, the 2A peptide cleavage efficiency of the multi-monitoring vector was confirmed by western blot analysis (Fig. S6, ESI†). And, we confirmed the phototoxicity by taking time-lapse images of multi-monitoring vector-transfected cells without anticancer drug as control cell (Movie.S1, ESI†)

In conclusion, we demonstrated a novel multi-imaging vector and validated its potential for monitoring cellular dynamics. Previous attempts to detect protein redistribution or trafficking of target molecules in live single cells required sample fixation and other treatments with antibodies or subcellular compartment labeling dyes. In contrast, the multi-imaging vector developed in this study can be used to express four distinct proteins in a single cell without performing chemical labeling, to stain the subcellular compartments or target proteins. Furthermore, this system would be able to express five proteins if another 2A peptide (P2A from PTV-1) is combined with the current 2A peptide. Finally, the combination of subcellular localizing signals and fluorescent proteins as labeling moieties in this 2A peptide system makes it possible to monitor complex cellular dynamics, such as apoptosis, using a conventional confocal microscope. It is important to design the vector appropriately to target subcellular organelles with fluorescent proteins according to the specific application needed. This robust imaging tool offers the ability to visualize complex cellular dynamics in live cells in real time, which could aid in drug development for disease treatment.

The authors acknowledge the financial support from BioNano Health-Guard Research Center funded by the Ministry of Science, ICT & Future Planning (MSIP) of Korea as a Global Frontier Project (H-GUARD_2013 M3A6B2078946) and the KRIBB Initiative Program.

Notes and references

1. W. V. Gilbert, *J. Biol.Chem.,* 2010, **285**, 29033.
2. M. Distel, J. C. Hocking, K. Volkmann and W. R. Köster, *J. Cell Biol.,* 2010, **191**, 875.
3. T. Weber and R. Köster, *Methods,* 2013, **62**, 279.
4. M. L. L. Donnelly, G. Luke, A. Mehrotra, X. Li, L. E. Hughes, D. Gani and M. D. Ryan, *J. Gen. Virol.,* 2001, **82**, 1013.
5. A. L. Szymczak, C. J. Workman, Y. Wang, K. M. Vignali, S. Dilioglou, E. F. Vanin and D. A. A. Vignali, *Nat. Biotech*., 2004, **22**, 589.
6. E. Provost, J. Rhee and S.D. Leach, *Genesis,* 2007, **45**, 625-629.
7. G. Trichas, J. Begbie and S. Srinivas, *BMC Biol.,* 2008, **6**, 40.
8. P. de Felipe, G. A. Luke, L. E. Hughes, D. Gani, C. Halpin and M. D. Ryan, *Trends Biotechnol*., 2006, **24**, 68.
9. D.M. Shcherbakova and V.V. Verkhusha, *Nat. Methods,* 2013, **10**, 751.
10. R. Rizzuto, M. Brini, P. Pizzo, M. Murgia and T. Pozzan, *Curr Biol.,* 1995, **5**, 635.
11. P. Adamson, H. F. Paterson and A. Hall, *J. Cell Biol*., 1992, **119**, 617.
12. D. Michaelson, J. Silletti, G. Murphy, P. D'Eustachio, M. Rush and M. R. Philips, *J. Cell Biol.*, 2001, **152**, 111.
13. D. Kalderon, B. L. Roberts, W. D. Richardson and A. E. Smith, *Cell,* 1984, **39**, 499.
14. J. H. P. Skene and I. Virag, *J. Cell. Biol*., 1989, **108**, 613.
15. E. C. Cheung, N. Joza, N. A. Steenaart, K. A. McClellan, M. Neuspiel, S. McNamara, J. G. MacLaurin, P. Rippstein, D. S. Park, G. C. Shore, H. M. McBride, J. M. Penninger and R. S. Slack, *EMBO J.,* 2006, **25**, 4061.
16. E. Norberg, S. Orrenius and B. Zhivotovsky, *Biochem. Biophys. Res. Commun.,* 2010, **396**, 95.
17. D. J. Smith, H. Ng, R. M. Kluck and P. Nagley, *IUBMB Life,* 2008, **60**, 383.
18. L, Cabon, P. Galán-Malo, A. Bouharrour, L. Delavallée, M-N. Brunelle-Navas, H. K. Lorenzo, A. Gross and S. A. Susin, *Cell Death Diff.,* 2012, **19**, 245.
19. S. P. Cregan, V. L. Dawson and R. S. Slack, *Oncogene,* 2004, **23**, 2785.
20. M. Loeffler, E. Daugas, S. A. Susin, N, Zamzami, D. Métivier, A. Nieminen, G. Brothers, J. M. Penninger and G. Kroemer, *FASEB J*., 2001, **15**, 758.
21. C. Muñoz-Pinedo, A. Guio-Carrión, J. C. Goldstein, P. Fitzgerald, D. D. Newmeyer and D. R. Green, *Proc. Natl. Acad. Sci. USA*., 2006, **103**, 11573.